



VIBRATION CONTROL OF A LARGE-SCALE TEST BUILDING USING HYBRID MASS DAMPER SYSTEM APPLIED ROBUST CONTROL THEORY

Morimasa WATAKABE¹, Osamu CHIBA² and Takayoshi KAMADA³

SUMMARY

The authors since 1990 have been working on the study and development of a vibration control system designed through use of Linear Quadratic optimal control theory (LQR). However, the LQR system needs many sensors, integrating amplifier, and cable to achieve vibration. To address these and other issues, as is well-known, robust control theory utilizes an efficient technique for vibration control of tall buildings. H_{∞} control theory and μ -synthesis, which are representative of robust control theory and are which reduce the vibration of a building using only the absolute acceleration of the roof floor, have robust stability and robust performance. This paper describes design of a control system based on H_{∞} control theory and μ -synthesis, as applied in an Active Mass Damper (AMD) system installed on a building. It has been demonstrated by simulations and observations that the designed controller has sufficient vibration AMD performance and robust performance under excitations.

INTRODUCTION

In recent years, the increasing number of high-rise buildings, sightseeing towers and other flexible and dynamically sensitive structures in Japan has generated increased interest in the field of structural vibration control¹⁾. This interest and awareness have manifested themselves in the construction of many structures equipped with vibration control systems to decrease building sway experienced by occupants. The authors have executed research and development of a new type of hybrid mass damper system using hydraulic actuators for response control of tall buildings since 1990 and have previously reported on response control performance of the AMD installed on a large-scale test building. Many of the control rules, which have been put to practical use, utilize state feedback with LQR. Relative velocity and relative displacement are used as a feedback signal for the amount of building deformation. However, the LQR system needs many sensors, integrating amplifier, and cable to achieve vibration. Although control performance was sufficient, reduction of costs of the control system was needed to make the system viable. An H_{∞} proposal with an effective control system design based on absolute acceleration measurement has previously been advanced to address these problems[1]. Previously, H_{∞} control theory

¹ Technical Research Institute, Toda Corporation, Tokyo, Japan. Email: morimasa.watakabe@toda.co.jp

² Technical Research Institute, Toda Corporation, Tokyo, Japan. Email: osamu.chiba@toda.co.jp

³ Tokyo University of Agriculture and Technology, Tokyo, Japan. Email: kama@cc.tuat.ac.jp

has been applied to design of the controller of an AMD system installed on a 6-story large-scale experimental building[2]. However, applying H_∞ control theory in conjunction with a real system causes problems. For example, control performance becomes conservative and performance gets worse when parameters fluctuate. On the other hand, with μ -synthesis, a perturbation is dealt with as a structured singular value instead of maximum singular value, therefore it can be used to evaluate robust performance. The reason is that H_∞ control theory overestimates error because a perturbation is dealt with as a maximum singular value. This control theory ended at an analytical level because it had been very highly developed, although there were very few practical use examples reported.

This paper describes the control system based on the robust control theory. The performance evaluation was considered from the time-history and the frequency area including previously a vibration control system designed through use of LQR. In addition, this paper presents the response control performance of the AMD system based on μ -synthesis obtained by simulation analysis and observation of behaviors during earthquake excitations

OUTLINE OF BUILDING AND AMD SYSTEM

Figure 1 shows a photo of the large-scale test building and the AMD installed on the roof of the building. The building on which the AMD system was installed was a steel truss tube structure with a 19 meter height, 470 tons total weight and a typical floor area of 8.8 x 8.8 meters. The first natural frequencies of the building in the X- and Y-directions are 0.73 and 0.84 Hz, respectively. The mass damper and accumulators are installed on the roof, while the hydraulic pump unit and controller are on the 6th floor. The responses of the building were recorded by velocity meters, which were set on each floor (6 sets, 12 components). Velocity and displacement transducers (2 sets, 4 components) were set on the damper. Table 1 summarizes the mass damper parameters. The moving mass has an outer size of $3 \times 3 \times 1.8^H$ meters. The moving mass weights of the AMD are 5.6 tons and 4.4 tons in the X- and Y-directions, respectively. The main mass is supported by a XY-motion mechanism, which provides free parallel movements in the horizontal directions. The main mass and intermediate frame form a moving mass in the X-direction. The main mass formed the moving mass in the Y-direction. The switching rule to either active or passive mode is determined by the system pressure and the mass displacement. The hydraulic actuator is mounted in each direction. The AMD system has two operational modes: the active mode and

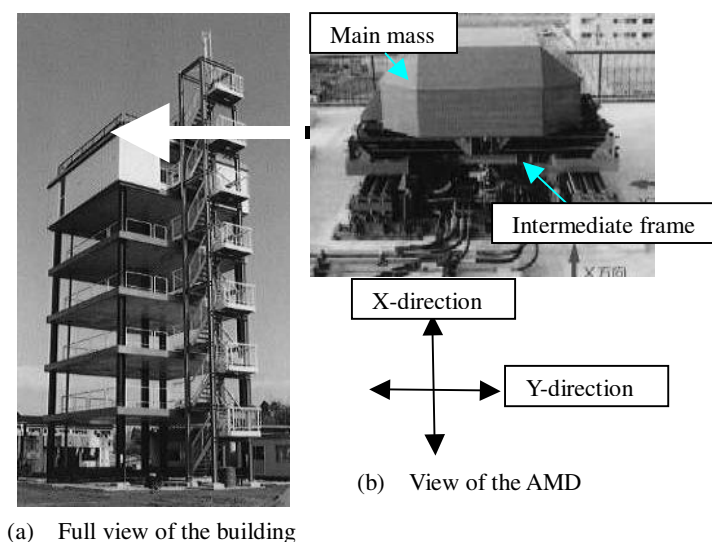


Figure 1. Large-scale test building and AMD

Table 1. Specifications of the AMD

	X-direction	Y-direction
Out size	3.0×3.0×1.8 ^H m	
Moving mass weight	55.9 KN	41.1KN
Effective mass ratio	2.2 %	1.6 %
Natural frequency	0.73 Hz	0.84 Hz
Maximum displacement	±35.0 cm	±35.0 cm
Friction coefficient	8/1000	12/1000
Pump unit	11.0 kW	
Accumulator	60.0 l	

the passive mode. The mass damper works actively to control the moderate vibrations caused by seasonal winds. It also works passively to control the large vibrations caused by strong winds or earthquakes. The control system operates independent of the x- and y- responses. The trigger signal and the hydraulic control ON/OFF signal, however, operate in conjunction with each other. This system monitors the absolute velocity of the roof or top floor of the building. If this measured value exceeds a threshold, the trigger signal is generated to start a control response. During the operation of the control mechanism, the system inputs the velocity and displacement of the mass damper, the actuator pressure, and the absolute acceleration of the roof or top floor into the personal computer via the A/D converter. The control voltage and the bypass opening signal are then computed and output is made to the hydraulic control panel through D/A conversion. The hydraulic control panel turns the hydraulic pump ON and OFF, opens and closes various valves, and detects certain system anomalies. The purpose of the AMD system is to reduce R.M.S. values of the response accelerations by about 1/3~1/2 during moderate seasonal winds under active control, and by about 1/2~2/3 during strong winds under passive control in comparison with response accelerations when vibrations are non-controlled.

ANALYTICAL MODELS

Analytical model of building and mass damper system

Figure 2 shows an analytical model of the building where the mass damper is installed on the roof. The building is assumed to have a shear-deformation mode in a 6-material point system in which the mass damper is located on the top floor. The X- and Y- directions are independently treated with a one-directional analysis model. The equations of the motion are represented as:

$$[M]\{\ddot{X}\} + [C]\{\dot{X}\} + [K]\{X\} = \{s\}[c_d\dot{x}_d + k_d x_d - ap] - [M][1]\ddot{z} + \{W\} \quad (1)$$

$$m_d(\ddot{x}_d + \ddot{x}_6 + \ddot{z}) + c_d\dot{x}_d + k_d x_d = ap \quad (2)$$

where $[M], [C], [K]$ (6×6) are respectively the building's mass, damping and rigidity matrices; $\{x\}$ (6×1) is the state vector and x_6 is the relative displacement vector of the roof or floor on which the mass damper is installed in comparison to the ground surface. \ddot{z} is the ground surface acceleration due to seismic

where: a is the piston's sectional area;

γ a constant indicating the rigidity of the cylinder; b is the flow-rate gain of the servo valve and u its input voltage; p_L is the load pressure of the cylinder; l^* is a reduction coefficient of output flow-rate due to servo valve internal leakage; and k_{fd} is the feedback gain to x_d .

The state equation is expressed as:

$$\dot{\mathbf{x}}_f = \mathbf{A}_f \mathbf{x}_f + \mathbf{b}_f u + \mathbf{h}_f \ddot{z} \quad (4)$$

Moreover, the output equation as the top absolute acceleration is expressed as

$$y = \mathbf{c}_f \mathbf{x}_f \quad (5)$$

As the objects of control, the 1st and 2nd mode vibration of the building was adapted. The following reduced-order is expressed as:

$$\dot{\mathbf{x}}_r = \mathbf{A}_r \mathbf{x}_r + \mathbf{b}_r u + \mathbf{h}_r \ddot{z} \quad (6)$$

$$y = \mathbf{c}_r \mathbf{x}_r \quad (7)$$

where “f” and “r” are respectively the same level model and the lower level model from equations (4) to (7). Furthermore, the building deflection equation of the control design uses equation (1) for the designed model up to and including the 2nd mode.

DESIGN OF CONTROLLER^{[5],[6]}

Generalized plant and weight function

The new control system was designed based on μ -synthesis, which is applied on the AMD system installed on the building. In the control system with μ -synthesis, a perturbation is dealt with through a structured singular value instead of maximum singular value. Accordingly, it can evaluate robust performance with robustness stability. Figure 3 shows the block diagram of generalized plant to which μ -synthesis is applied. Figure 3 shows a block line chart of the expanded control system, which contains disturbance and the weight function. The control system is treated as a correction mixed sensitivity issue by which disturbance was added to the input edge, and the control value, sensitivity by the output edge, and an addition error were evaluated. Initially, the part in one point chain line in Figure 3 can be expressed in the next equation:

$$\begin{Bmatrix} z \\ e \\ y \end{Bmatrix} = \mathbf{G} \begin{Bmatrix} w \\ d \\ u \end{Bmatrix} \quad (8)$$

where P_r is the design model, K is a controller; W_s and W_a are the weight function; Δ structured uncertainty, w and d are disturbance, z , e are controlled values, and u its input voltage; y is the output.

Using the I/O of equation (8), sensitivity function S and complementary sensitivity function T are expressed as:

$$e = Sd \quad (9)$$

$$z = Tw \quad (10)$$

H_∞ control applies to the weight functions of each factor because S of the above equation and T are the transfer functions from turbulence to the amount of control to do loop molding and to obtain the control machine which adjusts H_∞ norm of the transfer function to one or less.

$$\|W_s S\|_\infty < 1 \quad (11)$$

$$\|W_a T\|_\infty < 1 \quad (12)$$

The nominal performance condition and the robustness stability condition equations (11),(12) are shown above respectively. However, there is the following trade-off problems between S and T.

$$S + T = 1 \quad (13)$$

Next, if M shown in Figure 3 is assumed a closed-loop system which contains control machine K, by combining the equations (9)~(10), the part enclosed with the dotted line is described as follows :

$$\begin{Bmatrix} z \\ e \end{Bmatrix} = \mathbf{M} \begin{Bmatrix} w \\ d \end{Bmatrix} \quad (14)$$

If the μ design method adjusts H_∞ norm of a small gain to the structured uncertainty perturbation to one or less, the robust performance is secured. Then,

$$\text{Sup}_{\|\Delta\|_\infty < 1} \|F_U(M, \Delta)\|_\infty < 1 \quad (15)$$

Equation (15) shows the robustness performance condition, and F_U is one, which is called linear fractional transformation. As mentioned above, the weight function greatly impacts the control performance of the

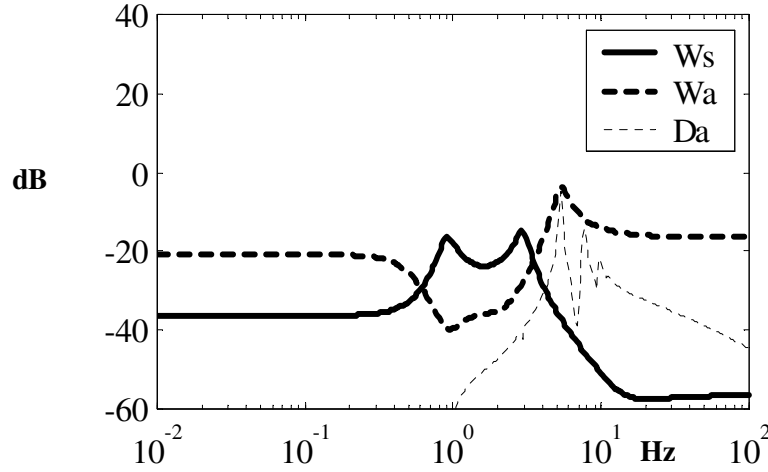


Figure 4. Weighting functions

robustness control theory. The weight function adopted for the H_∞ control and the μ design method are shown in Figure 4. Addition error Δ_a , which is derived from a comparison of the two models, namely the full model and the lower model, as expressed below:

$$\Delta_a(j\omega) = P_f(j\omega) - P_r(j\omega) \quad (16)$$

W_a is adopted for Δ_a in order to remove spillover instability of higher residual modes. The state equation of the low pass filter is expressed as:

$$|\Delta_a(j\omega)| \leq |W_a(j\omega)|, \quad \forall \omega \quad (17)$$

W_a is expressed as:

$$W_a(s) = k_a \frac{(s^2 + 2\zeta_{a3}\omega_{a3}s + \omega_{a3}^2)(s^2 + 2\zeta_{a4}\omega_{a4}s + \omega_{a4}^2)}{(s^2 + 2\zeta_{a1}\omega_{a1}s + \omega_{a1}^2)(s^2 + 2\zeta_{a2}\omega_{a2}s + \omega_{a2}^2)} \quad (18)$$

A superior filter characteristic in the first and second mode was given so that W_s might decrease

sensitivity from the ground acceleration to the roof or uppermost floor acceleration in consideration of the trade-off with W_a (Figure 4). W_s is expressed as equation (19).

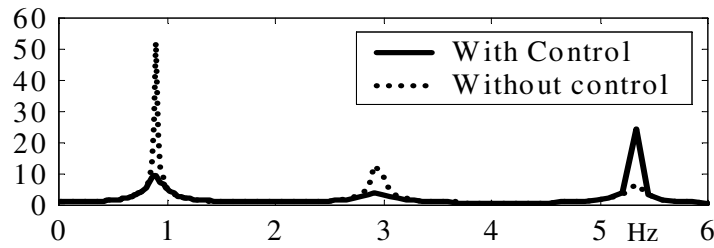
$$W_s(s) = k_s \frac{(s^2 + 2\zeta_{s3}\omega_{s3}s + \omega_{s3}^2)(s^2 + 2\zeta_{s4}\omega_{s4}s + \omega_{s4}^2)}{(s^2 + 2\zeta_{s1}\omega_{s1}s + \omega_{s1}^2)(s^2 + 2\zeta_{s2}\omega_{s2}s + \omega_{s2}^2)} \quad (19)$$

And ω_s , ω_a , ζ_s , ζ_a are the circular frequency, the attenuation ratios, k_a and k_s that wearing is arbitrary are the coefficient weights.

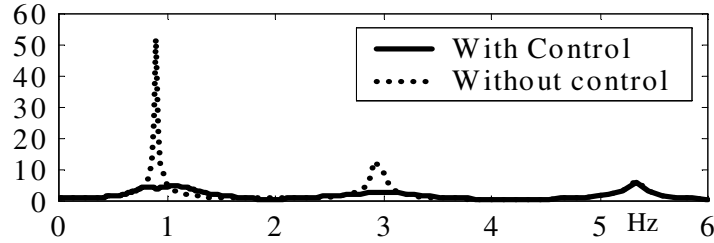
To become equivalent to a general value, the mode attenuation ratio 10% per first, and the mode attenuation ratio 5 % per second mode in the control device, the target control performance was selected.

Verification of controller performance

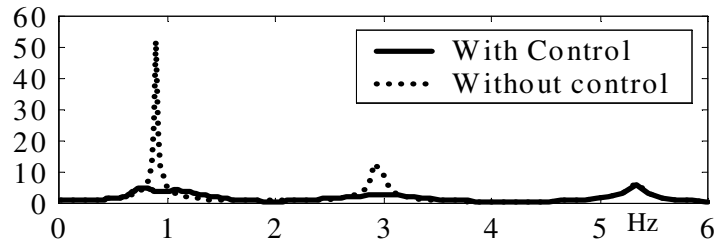
Next, the controller designed by the optimal regulator and the H_∞ control were compared by the transmission function to verify the control performance and the robustness of the μ controller as shown in Figure 5. The performance decreased because design and some parameters of the building model are different though LQR is the one that the first mode attenuation ratio was designed to become 14%. Moreover, the third mode has amplified by the parameter changes. Because the H_∞ control and the μ design kept the same target attenuation ratios, a big difference was not seen by both parties. The sensitivity functions are shown in Figure 6. There is a



(a) LQR Control



(b) H_∞ Control



(c) μ Control

Figure 5. Transfer function from ground acc. to roof-floor acc.

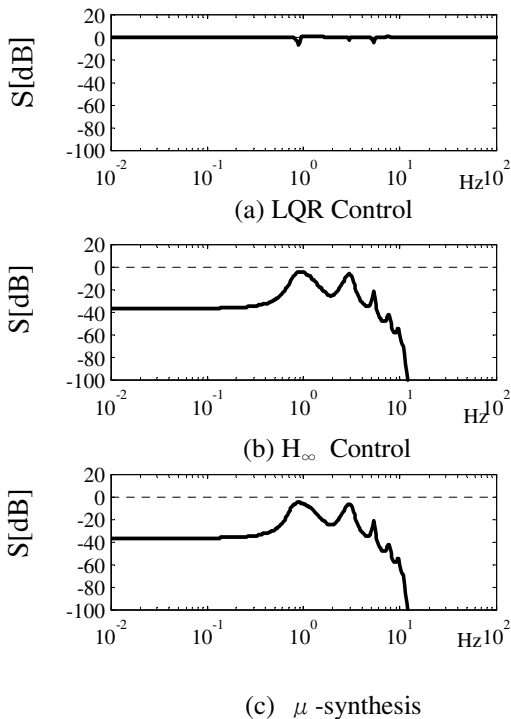


Figure 6. Sensitivity function

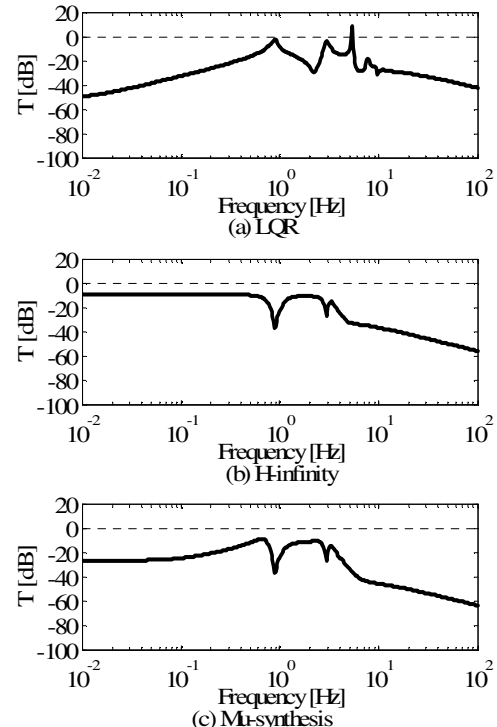


Figure 7 Complementary sensitivity function

part, which has exceeded 0dB because there is a parameter change though LQR suppresses the sensitivity function to 0dB or less in theoretical and all frequency band regions. In the robustness control, Figure 8 indicates the structured singular value. Both the structured singular values fall below 0dB intended for the control device as shown in Figure 8, though they deteriorate when 0dB exceeds the robustness performance because the demanded control performance is somewhat weak.

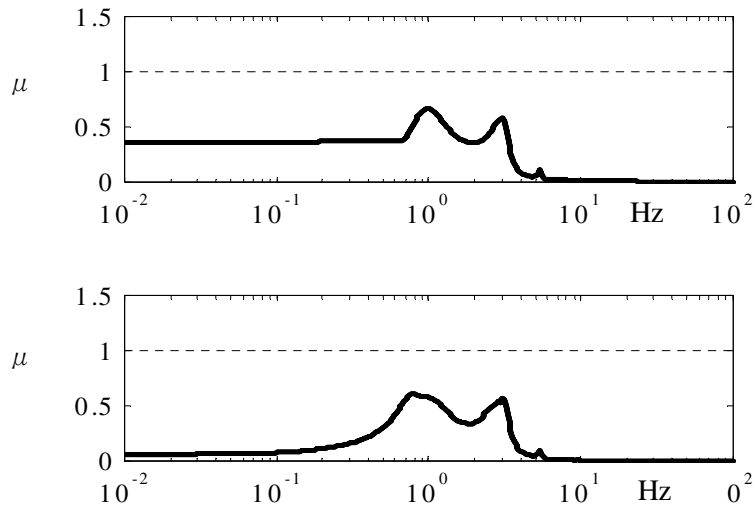


Figure 8. Structured singular value

Therefore, the advantage, using the μ -synthesis, can be called the control system design securing the robustness performance. However, the structured uncertainty is, in a word, tight control performance and improvement of robustness stability. In addition, because the latter has a low μ value overall if the

H_∞ controls are compared with the μ -synthesis, it can be said that it is a control system with high robustness or more performance.

RESPONSE CONTROL PERFORMANCE BASED ON OBSERVED RECORDS

Observation of behaviors in the event of some earthquake excitations has been carried out to investigate the response control performance of the AMD system based on μ -synthesis. Response observations of this actively controlled system were recorded for some actual earthquakes. The control response performance of the AMD system was investigated by comparing the responses for controlled and non-controlled states during earthquake excitations. The response spectra of the first floor acceleration records observed with the Off-shore Ibaraki Prefecture Earthquake (December 5, 2000) are shown in Figure 9. The JMA seismic intensity in constructed site was III, which was not so great.

Simulation analysis results of the response wave-forms for the roof and responses of the AMD in the Y direction installed on the structure building under the earthquake are shown together with observed results in Figure 10. Figures 10 (e), (f) and (g) indicate the control voltage and mass damper response in Y direction for active control. When the mode is active control, the control voltage and mass damper response increases and the sway response of the building is lessened. The simulation results also show good agreement with the observation, in magnitude and the time at which the maximum response occurs. The simulation for observation substantially verifies the validity of the employed analytical method and the modeling of the structure-AMD control system. It was confirmed that the response control effect can be estimated using the presented analytical method and model. According to these figures, the analytical and observed results agree well with respect to both structure responses and AMD responses, and the appropriateness of the analysis technique is verified. Figures 10 (b) and (d) show acceleration of the roof when non-controlled and controlled. The compared response results were observed data when controlled and simulated one obtained by response analysis when non-controlled, respectively. The damping ratio used in the analyses was assumed to be 0.5% when non-controlled. The peak value of the displacement under the active control is reduced to about 1/3 of that when non-controlled, and effectively suppressed the residual vibration of the building.

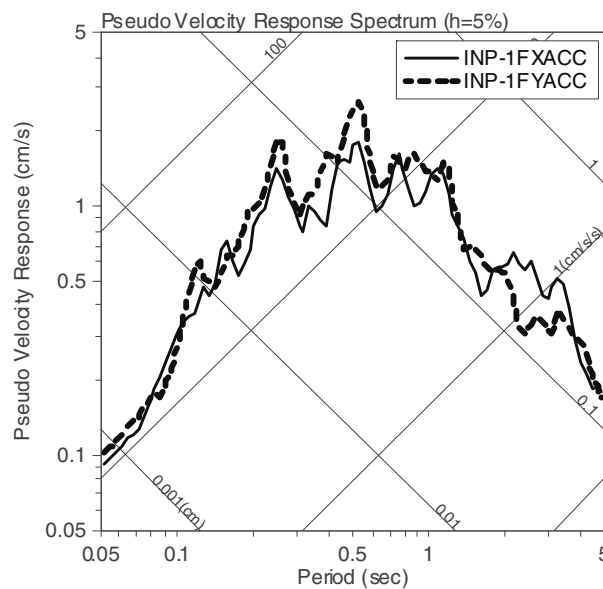


Figure 9. Acceleration response spectrum of 2000.12.05 Earthquake

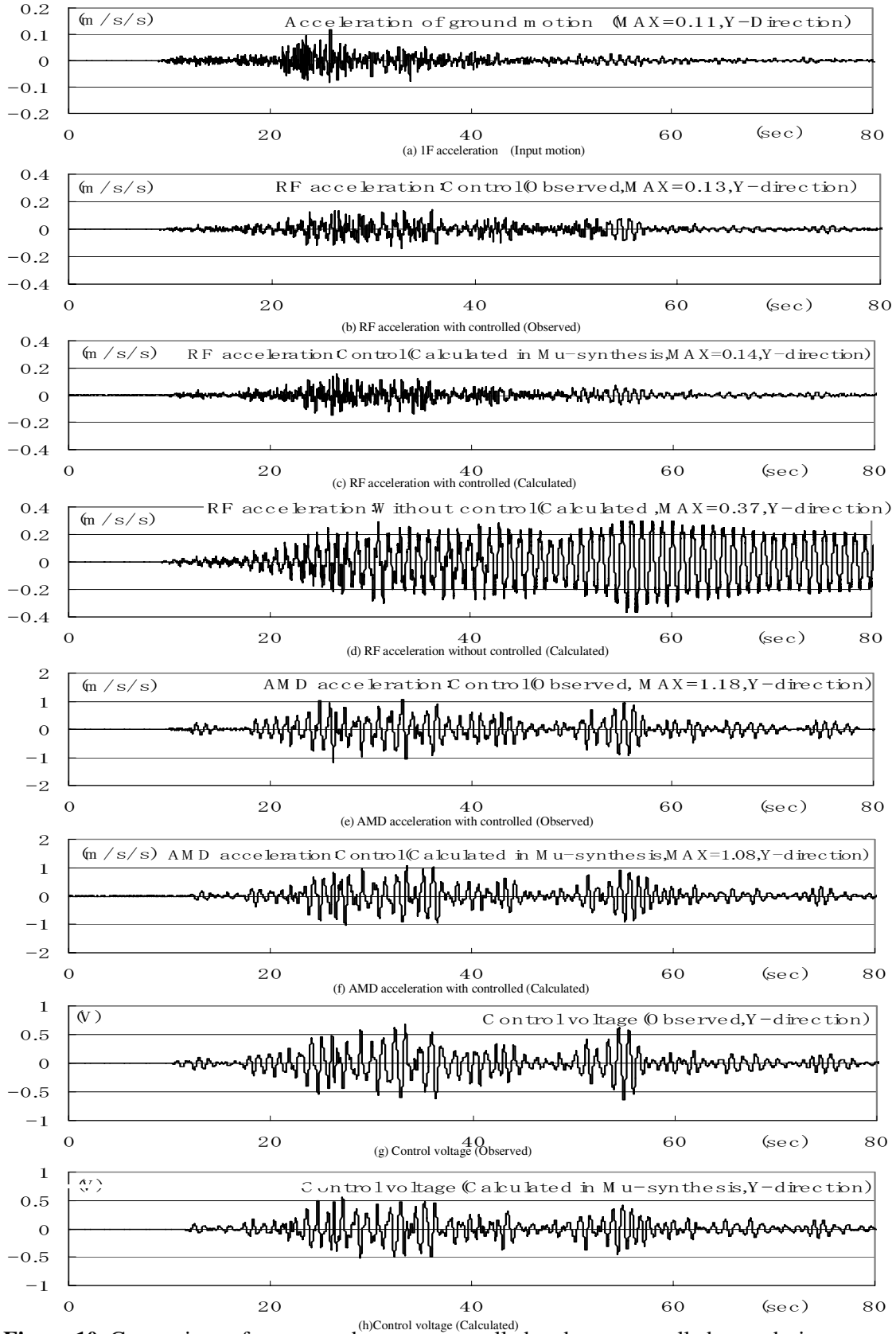
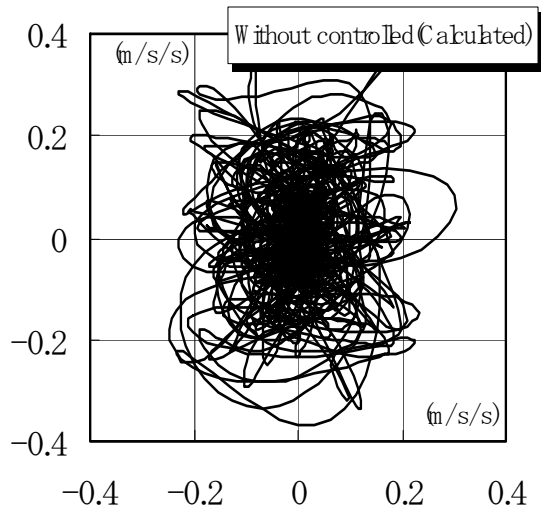
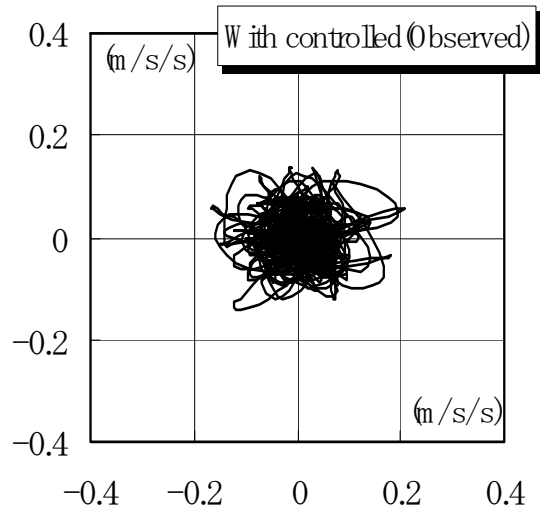


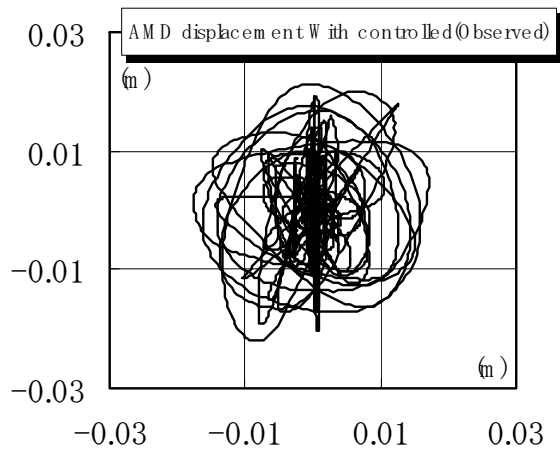
Figure 10. Comparison of responses between controlled and non-controlled state during earthquake measured record with calculated result in Y-direction



(a) Calculated result (Non-controlled)



(b) Observed result (Controlled)



(c) Observed response of the AMD (Non-controlled)

Figure 11. Comparison of Lissajous diagrams of the roof floor when the non-controlled and controlled

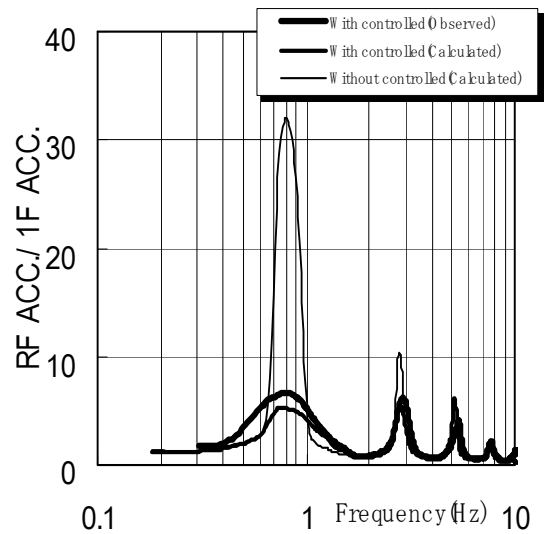


Figure 12. Transfer function from ground acceleration to roof-floor acceleration in Y-direction

The Lissajous diagram of the roof acceleration records in both the X- and Y directions when controlled as compared with non-controlled, is shown in Figures 11(a) and (b). The Lissajous diagram of the X and Y responses when controlled shows behavior similar to a circle, and then confirms that the damper response sharply increases and the (sway) response of the building lessen instantaneously. The transfer functions of the roof acceleration to the 1st floor input acceleration is shown in Figure 12.

The first natural frequencies of the building in the Y- directions obtained by the transfer function when non-controlled was about 0.73Hz. The response amplification factors at the 1st resonance peak when controlled were reduced to about 1/4 of that when non-controlled, and no spillover in the 2nd mode occurred. Though the earthquakes were weak, from these results the control effect during earthquake excitations was verified.

CONCLUSIONS

This paper describes design of a control system based on H^∞ control theory and μ -synthesis, as applied in an AMD system installed on a building. Simulation analysis and the observation of the behaviors during earthquake excitations were carried out to investigate the response control performance of the AMD applied robust control theory. It has been demonstrated by simulations and observations that the designed controller has sufficient vibration AMD performance and robust performance under excitations. Conclusions obtained are as follows;

- 1) The control system design using the robustness control theory was able to operate effectively utilizing only a single sensor for the first and second mode.
- 2) The robustness control system had high robustness (robustness stability and robustness control performance), though robustness stability degenerated greatly due to the change between the difference of the design model and the cycle etc., with respect to the LQR. It was shown to apply the μ design method to the control system design of AMD, and excellent in respect of the robustness stability and the robustness performance compared with the best regulator and the H_∞ control by the simulation analysis.
- 3) From the earthquake response observation record, the control system based on μ -synthesis demonstrated sufficient response control and high robustness.

ACKNOWLEDGEMENTS

This paper was supported by Mr. Jyunji Yamagami Graduate School of *Tokyo University of Agriculture and Technology* (Presently: Honda Motor Co., Ltd.). This support is gratefully acknowledged.

REFERENCES

1. View of design of dynamic turbulence,(in Japanese), Architectural Institute Japan, pp354-365,1996.11.
2. Yamada N.,Nishitani, A. H^∞ A Structural Control Design Based on Absolute Acceleration Measurement,(in Japanese and English abstract),pp49-58, No.484,Jurnal of structural and construction Engineering,1996.6
3. Watakabe, M.,Chiba O.,Ebisawa H.,Kamada T. and Yamagami A. Response control performance of active mass damper based on H^∞ control theory applied to a large-scale experimental building,,(in Japanese and English abstract),pp375-380, vol.46B,Jurnal of structural Engineering,2000.3
4. Nakatsuru, T., Iba D., Sone A. and Masuda A. Vibration Control of Structure by μ -Synthesis using tuned mass damper,(in Japanese and English abstract),pp65-70, Proceedings of the Second Japan National Symposium on Structural Control,2000
5. Nonami, K. and Qi-fu FAN (1994) Computer-Aided Control System Design and Control Performance for Active Vibration Control Systems with μ -Synthesis Theory, The Japan Society of Mechanical Engineers,(in Japanese and English abstract),pp77-83,60-572C,1994.
6. Nonami, K. and Qi-fu FAN ., The Japan Society of Mechanical Engineers,(in Japanese and English abstract),pp60-72,58-548C,1992
7. Fujita, T.,Mizuta, M.,Matsumoto, K., Kinoshita, M., Takanashi, S. and Miyano, H. (1993) Large-Scale Model Experiment of a Hybrid Mass Damper with Convertible Active and Passive Modes for Vibration Control of Tall Buildings, The Japan Society of Mechanical Engineers,(in Japanese and English abstract),pp36-43,59-557C,1993.